Development of an algorithm for assessing canopy volumes with terrestrial LiDAR to implement precision spraying in vineyards

A. Pagliai[1,*], D. Sarri[1], R. Lisci[1], S. Lombardo[1], M. Vieri[1], C. Perna[1], G. Cencini[1], V. De Pascale[1] and G. Araújo E Silva Ferraz[2]

[1]University of Florence, Department of Agriculture, Food, Environment and Forestry (DAGRI), Piazzale delle Cascine 15, IT50144 Florence, Italy
[2]Federal University of Lavras (UFLA), Department of Agricultural Engineering, Campus Universitário, PO Box 3037, CEP 37200-000 Lavras, Minas Gerais, Brazil
[*]Correspondence: andrea.pagliai@unifi.it

Abstract. Precision spraying is one of the techniques for the reduction of pesticides use and it can help achieve the new European Green Deal standards. The aim of such technique is to apply the right amount of pesticides according to the target characteristics. The precision spraying implementation requires target volume assessment, which can be carried out by LiDAR sensors. Such technique requires complex and time-consuming procedures of canopy characteristics computing through post-processing points cloud reconstruction. The present work aimed to develop and test an algorithm through the use of a tractor-coupled with terrestrial LiDAR and GNSS technology in order to simplify the process. With the aim to evaluate the algorithm the LiDAR-based volume was correlated with two manual measurements of canopy volume (Tree Row Volume and Point Net Cloud). The results showed good correlations between manual and LiDAR measures both for total canopy volumes ($R^2 = 0.67$ and 0.56) and for partial canopy volume ($R^2 = 0.74$). In conclusion, although the LiDAR-based algorithm works in automatic mode, the canopy volumes approximation seems acceptable to estimate the canopy volumes, with the advantages of a swifter procedure and less laborious post-processing computations.

Key words: canopy management technique, canopy measurements, site-specific data, variable rate technique, viticulture.

INTRODUCTION

In the last few decades, the public authorities focused their attention on reducing pesticide use and/or improving the efficiency of spraying operation (European Parliament, 2009; MIPAAF, 2014). The European Commission has recently declared that it is essential to introduce coherent strategies to halve the use of chemical pesticides by the year 2030 (ECP, 2020). Variable rate applications (VRA), telemetry of crop protection stages, integrated pest management (IPM) and decision support systems (DSS) can be effective strategies to achieve the European goals. VRA consists of variable-rate spraying according to the characteristics of the canopy (height, width, volume, leaf area, leaf density) or vigour index (Miranda-Fuentes et al., 2016; Tsoulias

et al., 2019; Cheraïet et al., 2020; Román et al., 2020). A 20–30% reduction in pesticide use has been achieved by detecting tree size and architecture, (EPRS, 2016). Other improvements have been reached by using auxiliary telemetry tools for crop protection phases (Sarri et al., 2020). In addition, the adoption of Integrated Pest Management (IPM) was able to reduce a sprayed area by approximately 50–80% (EPRS, 2017).

The variable-rate application technique consists in obtaining similar plant protection products (PPP) deposits according to canopy characteristics (Gil et al., 2013). To fulfil the variable-rate applications, canopy dimensions have to be measured. Originally, canopy measurement was carried out manually and the corresponding canopy indicators were created (Tree Row Volume, Leaf Area Index, Leaf Wall Area, Unit Canopy Row, Ellipsoid Volume Method) (Pergher & Petris, 2008; Miranda-Fuentes et al., 2015). Obtaining these manual indicators was time-consuming. Gradually, thanks to technological development, faster and more efficient measurement methods have been developed (Rosell & Sanz, 2012; Comba et al., 2019). Several studies have used ultrasonic sensors to improve variable-rate application (Llorens et al., 2010; Llorens et al., 2011, Gil et al., 2013). These sensors operate with ultrasonic waves, and provide a precise assessment of canopy width in small portions of vegetation. Improvements of canopy detections were provided by LiDAR (Light Detection and Ranging) sensors. The LiDAR technology works with laser beams, and it provides canopy point cloud, at various angular resolution and various aperture angle (Rosell & Sanz, 2012). Thus, the entire vertical profile of the canopy can be reconstructed. Many studies were carried out for implementing the LiDAR-based canopy measurements (Palacín et al., 2007; Rosell et al., 2009a; Llorens et al., 2011; Sanz et al., 2013; Miranda-Fuentes et al., 2015; Tsoulias et al., 2019). Some works obtained canopy characteristics with complicated and laborious steps that required a great amount of post-processing operations. In other works it was necessary to carry out point cloud reconstruction and data filtering to obtain a correct and precise canopy characterization. Only after these operations it was possible to run the canopy parameters computing. Although they are valid methods for research domains, these procedures do not coincide with the implementation of variable-rate operations during work operations. The data extract must be well suited with the tractor speed during spray operations to implement VRA. Therefore, for data processing, few milliseconds are usable. Moreover, the accuracy of canopy measurements, reached by post-processing operations is often too high for practical purposes. Very few studies were focused on practical and operative tools for assessing canopy volumes in real time (Zhang et al., 2018). It is thus evident that a functional LiDAR-based tool is needed to optimise the variable-rate application of pesticides in viticulture. A procedure for automating the LiDAR-based canopy volume computing in real-time was developed to reach this target.

Therefore, this paper focuses on the development and testing of a LiDAR-based algorithm and software for the automatic calculation of canopy volume using a tractor-coupled with terrestrial 2D LiDAR and GNSS receiver.

In order to check algorithm and software, a number of comparison tests were carried out between two different manual canopy volume measurements and LiDAR canopy volume measurements. The experimental tests were carried out in two vineyards, with different row spacing and plant density parameters. Finally, the canopy volumes of four vine-rows, which were completely travelled, were analysed in two work sessions to check the software functioning during the different growth stages.

MATERIALS AND METHODS

Instrumentations:

The 2D LiDAR Sick TIM561 was used (Fig. 1, a) to perform the study. The main sensor features were an angular resolution of 0.33°, an aperture angle of 270°, a working range from 0.05 m to 10 m, a laser emission wavelength of 850 nm and a scanning frequency of 15 Hz (TIM561 Sick). Thanks to these characteristics, 12,150 points were captured each second.

Moreover, to obtain geo-referenced data, the 2D LiDAR was coupled with Ag Leader GPS6500 GNSS receiver (Fig. 1, b). This GNSS receiver provides differential correction with a horizontal position accuracy of 0.4 m, a velocity accuracy of 0.03 m s^{-1} and a maximum data rate of 50 Hz (GPS 6500, Ag Leader).

The LiDAR sensor and GNSS receiver were connected together through a Panasonic Tough Pad FG-Z1, where the algorithm and software for calculating the canopy volume were installed (Fig. 1, c).

Figure 1. Instruments assembled during a field test session with details of the individual tools used (a) GNSS receiver; b) LiDAR sensor; c) Panasonic computer).

During field tests, all these instrumentations were mounted on a Kubota B2420 tractor. On the one hand, the Panasonic computer and the GNSS receiver were assembled near the steering station. On the other hand, the 2D LiDAR was positioned in the rear of the tractor in a vertical position to correctly scan the vertical profiles of the canopy, thanks to 270° opening angle.

Algorithm and Software:

The calculation of the canopy volume was made using an algorithm for extracting the canopy contours, integrated into software for real-time visualisation of the canopy volumes and its main characteristics. In addition, the software creates a comma-separated values (CSV) file-data where the volumes of canopies, associated with their global position (EPSG:4326-WGS 84), and working parameters of the tractor (speed, distance between scan$_i$–scan$_{i+1}$) were recorded.

It is worth noting that before starting the data acquisition, the GNSS acquisition frequency can be changed from 0.1 to 15 Hz in the software interface page.

Its frequency rate controlled the entire exchange of data. Specifically, each time the GNSS string arrived, it was processed by software that sent a data request to the LiDAR. Instantly, a LiDAR scan was run, processed and recorded (with an angular resolution of 0.33° and a scan range of 270°). This process was reiterated until the data acquisition end. For the transfer of LiDAR data, an ethernet connection was used. Instead, an RS232 serial port was used for GNSS data transfer.

First of all, row data provided by LiDAR sensor were transformed from polar to cartesian coordinates. The transformation was made for all points individuated by LiDAR sensor in a single scan (angular resolution: 0.33°; aperture angle: 270°;
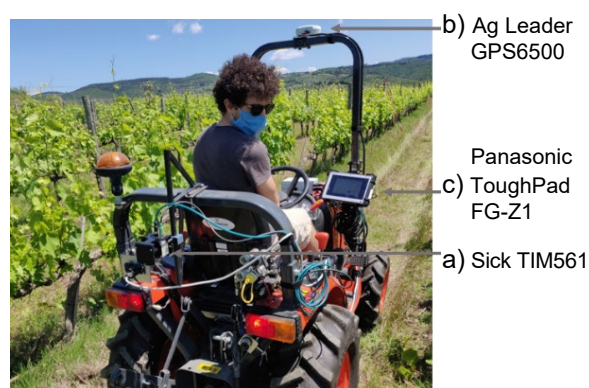
maximum point for single scan: 810) and for all scan frequency (scan frequency: 15 Hz = 15 scan s^{-1}), using the following formula:

$$C\_xy_{ij} = \begin{cases} X = DV_{ij} * \cos \alpha_{ij} \\ Y = H_{Li} + DV_{ij} * \sin \alpha_{ij} \end{cases} \tag{1}$$

where C_xy_{ij} – detected canopy point in cartesian coordinates; DV_{ij} – distance between LiDAR and canopy at determined angular position j and the moment i; α_{ij} – angle subtended by DV_{ij}; H_{Li} – LiDAR average height from ground-level. Graphically representation is shown in Fig. 2.

Then, if X coordinates of the canopy points (C_xy_{ij}), that corresponded to the distance between LiDAR and canopy in the cartesian system, were equal or bigger than semi row spacing ($D_{rs}/2$), they were considered in the calculation of canopy volume as values 0, because these points did not belong to the canopies near the tractor. In comparison, laser beams that did not encounter any obstacles were not counted. Moreover, another condition had to be respected. The Y coordinates of the canopy points (C_xy_{ij}) must be bigger than H_{co} (average cordon height). In this way, the points detected in the ground-level or other interferences, as grass or vine trunk, were not considered. Thanks to LiDAR characteristics (TIM561 Sick), particularly the aperture angle of 270°, it was possible to detect two sides of vine-rows for each working route. Therefore, the conversion formula and the conditions previously exposed were viable for both sides of vine-rows (Fig. 2, left side).
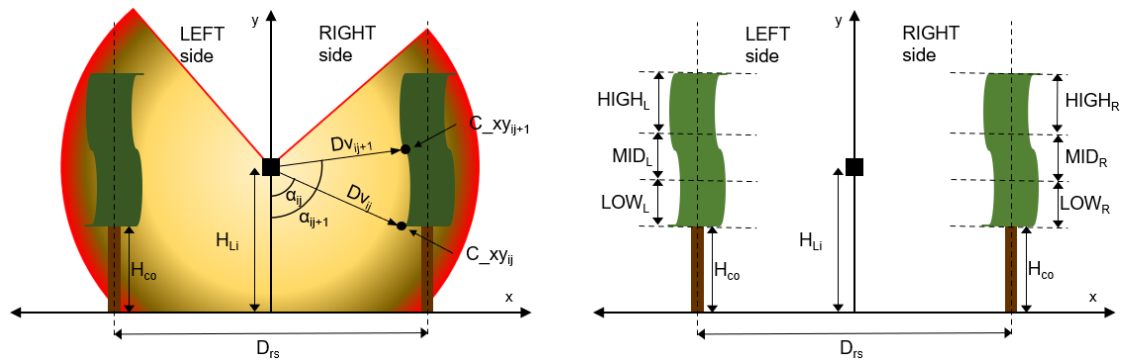

Figure 2. In the left side of the figure, the LiDAR and algorithm working principles were represented. In the other side, the subdivisions in three bands were shown.

A subdivision of total canopy volume in three bands according to the height from cordon was carried out. Specifically the low band was between the cordon (H_{co}) up to 0.30 m in vertical height (H_{co+30}), the middle band was between the end of the previous one up to 0.60 m apart the cordon (H_{co+60}) and the high band was between the end of the previous one up to the last canopy detected point ($ymax$) (Fig. 2, right side). The subdivision in three bands was necessary to discriminate how the canopy arranges on the vertical profile. Without these partitions, only the total canopy volume would have been measured and it would not have been possible to show the differences in the vertical profile of the canopy.

Then the algorithm, according to different canopy bands, computed total and partial means of the x-values of canopy points (C_xy_{ij}). To differentiate the three bands, the y-values of canopy points (C_xy_{ij}) were used. These average values ($\overline{X_{tot}}$; $\overline{X_{high}}$; $\overline{X_{mid}}$; $\overline{X_{low}}$) correspond to distance between LiDAR and canopy in a different portion of canopy profile. The subtraction between semi row spacing ($D_{rs}/2$) and average values were done to obtain both total average canopy width and partial average canopy widths (low, mid and high canopy bands). Finally, the entire and partial areas of canopy sections were obtained by the multiplication between their widths and heights. In such a manner, the canopy areas (m^2 scan^{-1}) of vertical LiDAR scan were obtained, both for left and right sides. The equations below showed the procedure aforementioned (2) (3) (4) (5).

$$\overline{X_{tot}} = \frac{\sum_{y=H_{co}}^{ymax} x_i}{n_t} \rightarrow A_{tot} = \left(\frac{D_{rs}}{2} - \overline{X_{tot}}\right) * (ymax - H_{co}) \tag{2}$$

$$\overline{X_{high}} = \frac{\sum_{y=H_{co+60}}^{ymax} x_i}{n_h} \rightarrow A_{high} = \left(\frac{D_{rs}}{2} - \overline{X_{high}}\right) * (ymax - H_{co+60}) \tag{3}$$

$$\overline{X_{mid}} = \frac{\sum_{y=H_{co+30}}^{H_{co+60}} x_i}{n_m} \rightarrow A_{mid} = \left(\frac{D_{rs}}{2} - \overline{X_{mid}}\right) * (H_{co+60} - H_{co+30}) \tag{4}$$

$$\overline{X_{low}} = \frac{\sum_{y=H_{co}}^{H_{co+30}} x_i}{n_l} \rightarrow A_{low} = \left(\frac{D_{rs}}{2} - \overline{X_{low}}\right) * (H_{co+30} - H_{co}) \tag{5}$$

where $\overline{X_{tot}}$, $\overline{X_{high}}$, $\overline{X_{mid}}$, $\overline{X_{low}}$ – average values of x coordinates, respectively for total canopy, high canopy band, mid canopy band and low band; H_{co} – cordon height; H_{co+30} – cordon height plus 0.30 m; H_{co+60} – cordon height plus 0.60 m; $ymax$ – the y coordinate of last canopy point detected by LiDAR; x_i – x coordinate in C_xy_{ij}; n_t, n_h, n_m, n_l – number of canopy points included respectively in total, high, mid and low canopy band; A_{tot}, A_{high}, A_{mid}, A_{low} – respectively total section area of the canopy and partial sections area (high, mid, low); ($D_{rs}/2$) – semi row spacing.

The first version of the algorithm had not division into three canopy bands. Nevertheless, during the early tests, it became necessary to highlight how the canopy arranges in the vertical profile. It has been essential for showing how the total canopy volume and the proportion of partial canopy volume, in the vertical profile, changed during the growing season.

The final algorithm step consisted in calculating the canopy volumes through the multiplication between the canopy area and travelled distance by tractor during a detection session. The travelled distance was obtained by GNSS receiver. The final output was a CSV file with canopy volumes (total and partial) linked with their global

$$V_{tot} = A_{tot} * D_t, \quad m^3 D_t^{-1} \tag{6}$$

$$V_{high} = A_{high} * D_t, \quad m^3 D_t^{-1} \tag{7}$$

$$V_{mid} = A_{mid} * D_t, \quad m^3 D_t^{-1} \tag{8}$$

$$V_{low} = A_{low} * D_t, \quad m^3 D_t^{-1} \tag{9}$$

positions, provided by GNSS receiver. The volumes of canopy can be obtained referring to the distance travelled (Eqs 6, 7, 8, 9) or to the linear meter of row (Eqs 10, 11, 12, 13).

$$V_{tot} = (A_{tot} * D_t) * \frac{1}{D_t}, \; m^3 m^{-1}$$

$$V_{tot} = (A_{tot} * D_t) * \frac{1}{D_t}, \; m^3 m^{-1} \quad (10)$$

$$V_{high} = (A_{high} * D_t) * \frac{1}{D_t}, \; m^3 m^{-1} \quad (11)$$

$$V_{mid} = (A_{mid} * D_t) * \frac{1}{D_t}, \; m^3 m^{-1} \quad (12)$$

$$V_{low} = (A_{low} * D_t) * \frac{1}{D_t}, \; m^3 m^{-1} \quad (13)$$

where V_{tot} – total canopy volume; V_{high} – high band canopy volume; V_{mid} – mid band canopy volume; V_{low} – low band canopy volume; D_t – distance travelled.

The algorithm carried out all calculations, both for left and right side of vine-rows, during a working session.

The algorithm was integrated into a software, designed to process LiDAR data automatically and in real-time. This software was implemented in Visual Studio with C# programming language. The software has an interface page, where parameters can be changed according to vineyards characteristics, and a working page, where canopy volumes and heights, positions and errors codes (about LiDAR) can be seen. On the first page, it was possible to change parameters such as row spacing, LiDAR height and cordon height from ground level. This allowed the setting into other vineyards (with different characteristics) or potentially into other crops for instance orchards. In the second window, the recording of the work session can be activated and, at the end of it, a CSV file is created. This output contains the main working parameters such as time, GNSS position and tractor speed, and canopy characteristics such as total canopy volumes, high band, mid band and low band canopy volumes for both the right and left side.

Figure 3. Software interface for computing, in real-time, canopy volumes. On the left, the interface window, that allows to set parameters about LiDAR position and vineyard characteristics was shown. On the right, there is the working window, where canopy volumes (right and left side) and canopy heights were shown in real-time.

Field tests:

The field tests were carried out in two different vineyards in Chianti Classico region. The first one was located in Gretole (43°27'23.0" N; 11°13'51.9" E), Castellina in Chianti, Siena, Italy and the other located in San Felice (43° 23' 24.8" N; 11° 27' 26.5" E), Castelnuovo Berardenga, Siena, Italy.

At the moment of tests, the vineyard in Gretole was 11 years old, was cordon trained, with a row spacing of 2.5 m and an average distance between vines of 0.8 m. With a plant density of ~5,000 vine ha^{-1}. San Felice's vineyard was cordon trained, it was 15 years old, and the plant density was higher than the first one (~9,000 vine ha^{-1}). It is due to a smaller row spacing (~1.4 m). Both vineyards were mainly composed of *Vitis vinifera* L. cv. 'Sangiovese'. During the 2020 vegetative season (May-July), three test sessions were carried out in three different phenological phases (BBCH 57, BBCH 71, BBCH 81), for a total of 26 vines sampled for each measurement technique. This was done to test whether the algorithm could work at very different inter-row distances, distinguish canopy growth during sprout's development, and differentiate canopy volume according to different vigour zones.

To check the algorithm two different types of manual non-destructive canopy measurements were carried out. The first manual measurements was the Tree Row Volume (TRV) which was measured for each single vines involved in the experiments. The TRV technique involved in this experiment was partially revised from conventional TRV to provide the volume of the canopy of each vine (m^3 plant^{-1}) (Scapin et al., 2015). This was achieved by computing the average canopy height (m), the average canopy width (m) and the average canopy length (m) of a single vine with the following Eq. (14).

$$TRV = \bar{H} * \bar{W} * \bar{L}, \text{(m}^3 \text{ pl}^{-1}\text{)} \tag{14}$$

where $\bar{H}$ – was the average canopy height; $\bar{W}$ – was the average canopy width; $\bar{L}$ – was the average canopy length; m^3 pl^{-1} – unit of measure.

The other manual measurements adopted was the Point Net Canopy (PNC). It consisted in measuring the canopy width for each mesh of the net, positioned in parallel to vineyard row and in front of the canopy surface (Fig. 4). The PNC provides more detailed canopy volume than TRV because several canopy width for each vine sampled were measured. To calculate the PNC, a net, with a mesh of 0.15 m × 0.15 m, was located to a distance of 0.5 m from vertical canopy axis. Then, the distance (d_i) between canopy external surface and net was manually measured for each mesh of the net. In addition, the value d_i was subtracted by the distance between the net and vertical canopy axis (0.5 m) in order to obtain canopy widths for each mesh of the net. This value was multiplied by the area of the mesh ($A_i = 0.0225$ m^2) to obtain the volumes of the canopy subtended by single meshes. Finally, they were added up to obtain the total volume of the canopy of a single vine, as follows in the Eq. (15).

$$PNC = \sum_{i=1}^{n} [A_i * (0.5\,m - d_i)], \quad \text{(m}^3 \text{ pl}^{-1}\text{)} \tag{15}$$

where d_i – distance between canopy external surface and net; A_i – mesh area; $0.5\,m$ – the distance between net and canopy vertical axis; i – number of meshes contained the sampled vine canopy.

PNC provides detailed information on the spatial distribution of canopy volume. In particular, canopy volumes for different vegetation bands (0–0.3 m; 0.30–0.60 m; and > 0.60 m; distance from cordon) can be extracted from this manual measurements. This was essential to correlate with the canopy volume bands provided by LiDAR algorithm.
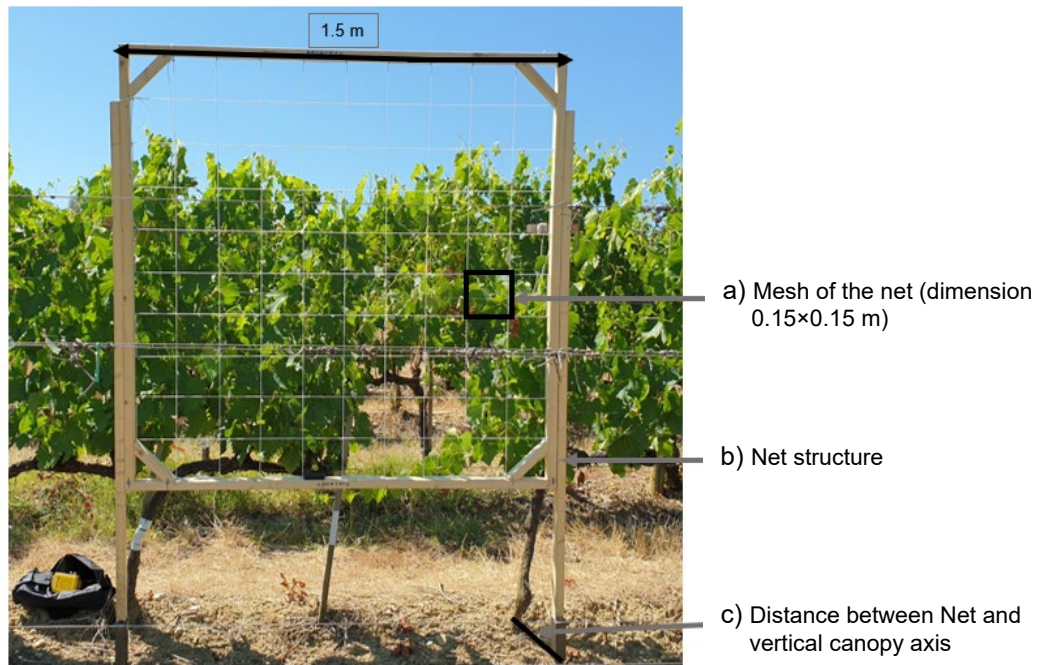

Figure 4. Net positioned for a manual measurement session. (a) Net mesh dimension; b) Net structure; c) Distance Net structure–Vertical canopy axis.

Finally, TRV and PNC measurements were compared with LiDAR measurements to validate the performance of the algorithm. The LiDAR measurements were carried out throughout vine-rows, containing the sampled vines, at an average speed of 1 m s^{-1}. The acquisition frequency was set up at 10 Hz, to obtain a scan each about 0.1 m. From these data, the LiDAR canopy volumes, corresponding to sampled vines manually, were extracted thanks to GNSS receiver and a digital marker that highlights sampled vines in the file output. The vine-rows, including the sampled vines, were travelled in their entirety in order to get the full characterisation of the canopy.

RESULTS AND DISCUSSION

Manually and LiDAR measurements on single vines:
As far as the canopy volumes of sampled vines, the minimum, average and maximum values for the three measurement techniques (TRV, PNC and LiDAR) were summarised in Table 1. In this table, canopy volume values, in different work sessions (May and July), were simultaneously shown to highlight how LiDAR measurements have detected the increasing of canopy volumes during the growing phase (from BBCH 57 to BBCH 81). The increase in canopy volumes was also identified by the other manual measurements. This suggest that the algorithm and software work well enough.

Table 1. Minimum, mean and maximum values of manuals and LiDAR measurements in the same plants at different growth stages (BBCH 57–BBCH 81)

	TRV		PNC		LIDAR	
	BBCH 57	BBCH 81	BBCH 57	BBCH 81	BBCH 57	BBCH 81
Min.	0.118	0.326	0.086	0.115	0.096	0.219
Mean	0.229	0.368	0.150	0.253	0.193	0.288
Max.	0.307	0.472	0.210	0.360	0.290	0.403

Two comparisons of total canopy volumes between instrumental and manually measurements to validate the LiDAR measurements were analysed. Linear regressions provide more evidence of the algorithm good functioning. This analysis highlights good correlations between TRV and LiDAR measurements ($R^2 = 0.67$) and PNC and LiDAR measurements ($R^2 = 0.56$), how it is shown in Fig. 5. The obtained linear regression (TRV *vs* LiDAR) has slightly lower coefficients of determination than other similar comparisons presented in some papers (Rosell et al., 2009b; Tsoulias et al., 2019). Indeed, Tsoulias et al. (2019) found a better coefficient of determination ($R^2 = 0.77$), under similar conditions and with the same experimental parameters, but this result was obtained with a significantly lower tractor speed. Instead, Rosell et al. (2009b) reported a better coefficient of determination ($R^2 = 0.97$), but this was obtained with a small sample size and in an apple orchard.
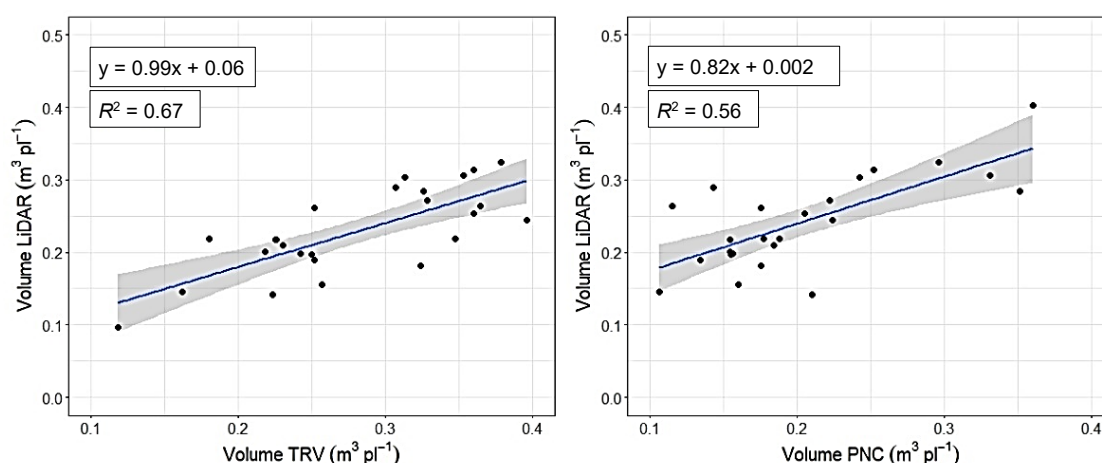

Figure 5. The linear regression of TRV (x) versus LiDAR (y) volume measurements is shown on the left graph. The linear regression of PNC (x) versus LiDAR (y) volume measurements is represented on the right chart.

This study wanted to test the automated assessment algorithm of canopy volume in operational working conditions, hence this could be the reason for obtaining smaller coefficients of determination. However, this approximation is justified because the tractor speed was set to the average speed for future software implementation in canopy management operations and variable-rate spraying applications.

With regard to canopy volumes divided into three bands, linear regressions between LiDAR and PNC measurements were obtained. The TRV measurements were not considered because the TRV method does not provide specific canopy information as vertical distribution of canopy volumes. LiDAR and PNC correlations for low and mid

bands reported similar determination coefficients, respectively 0.498 and 0.491 (Fig. 6). Instead, the coefficient of determination for the high band, i.e. the portion of the canopy between a distance of 0.60 m from cordon height and the last canopy point detected by LiDAR, is 0.736, as shown in Fig. 6. The differences in coefficient of determination between the canopy bands are probably due to the dimension of bands. In fact, the high band includes a portion of canopy bigger than other bands. So, this brings about the values of the canopy of high band (m3 pl-1) being bigger than those of the mid and low band. Therefore, slight deviations between PNC and LIDAR measurements in the high band cause a minor deterioration of the coefficient of determination compared to what happens in low and mid bands, where the values of the canopy are smaller.
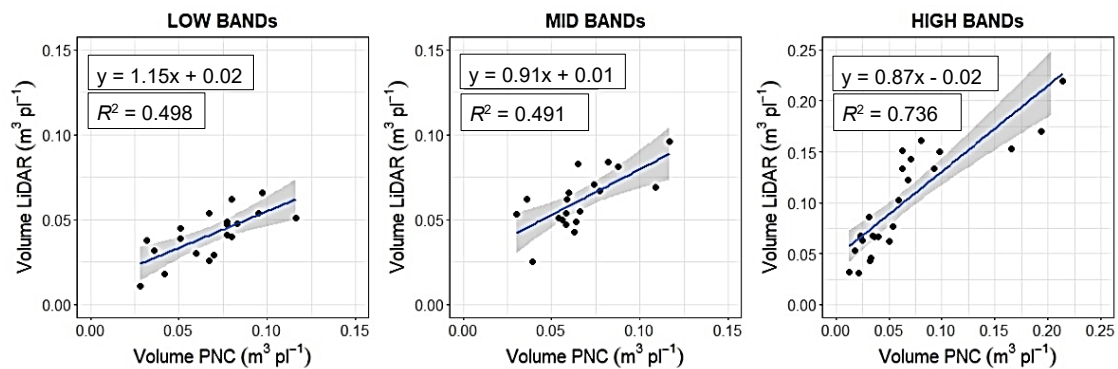

Figure 6. The linear regressions of PNC (x) *versus* LiDAR (y) volume measurements are shown with the detail of the three canopy bands (on the left: Low Band; in the middle: Mid Band; on the right: High Band).

However, this value highlights a good approximation provided by the algorithm for automated canopy volumes computing. This information is essential in future developments of precision spraying. In fact, the total canopy volume based on LiDAR is an excellent index to assess the spatial variability in terms of canopy quantity in vineyards. Thanks to the total canopy volume, the pesticides spray volume can vary according to site-specific information. Moreover, the spray volume can be targeted according to the vertical canopy variability, due to the division of the canopy into bands.

The significant correlation obtained in the high canopy bands is another interesting aspect to be evaluated more carefully. Indeed, the computation of canopy high bands could potentially be affected by less accuracy due to slight lateral inclinations of vineyards or tractor roll motion. Nevertheless, they do not seem to be problematic in the canopy volume approximation. Therefore, the algorithm gives a good approximation of the total canopy volume and provides helpful information about the vertical distribution of canopy volumes.

LiDAR measurements of entire vineyards

The canopy volumes detected by LiDAR software during two working sessions (May and July) were showed. The data represent the canopy volumes ($m^3 m^{-1}$) of four vine-rows completely travelled at a constant tractor speed of 1 ms^{-1}. This situation simulated the usual working conditions of canopy management.

The absolute frequency of total canopy volumes partitioned in breaks of 0.01 m^3 m^{-1} during the evolution of total canopy volumes from BBCH 57 stage to BBCH 81 was showed in Fig. 7.
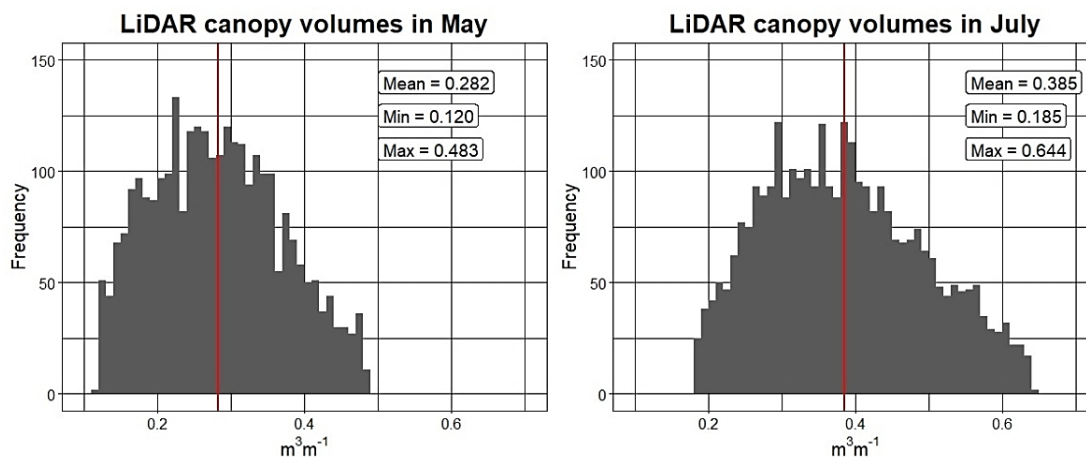

Figure 7. Absolut frequencies of LiDAR measurements with a interval of 0.01 (m^3 m^{-1}). Such measurements were part of the software output (CSV file) where tractor, coupled with LiDAR, travelled completely four vine-rows. The red line corresponds to the mean value.

In BBCH 57 stage, an average canopy volume of 0.282 m^3 per linear meter of vine-row was detected, with a minimum value of 0.120 m^3 m^{-1} and a maximum of 0.483 m^3 m^{-1}. Instead, in BBCH 81 stage, an average canopy volume of 0.385 m^3 m^{-1} was measured, with a minimum of 0.185 m^3 m^{-1} and a maximum of 0.644 m^3 m^{-1}.

The increase in canopy volume (from 0.282 to 0.385 m^3 m^{-1}) between the two phases was 37% reflecting thenatural growth phase of the vineyard, as shown in Table 2. This increase was also detected by the two manual canopy measurements (Table 1). Therefore, the algorithm for the automatic calculation of canopy volumes was able to detect the different canopy volumes during the growth phase of the vineyard.

Table 2. Means of canopy volumes of LiDAR measurements, percentage of canopy distribution between bands and rate of volume increase between different growth stages (BBCH 57 – BBCH 81)

	BBCH 57		BBCH 81		BBCH 57 – BBCH 81
	Mean	%	Mean	%	%
Tot	0.282		0.385		37%
High	0.1565	61%	0.205	60%	31%
Mid	0.0598	23%	0.0834	24%	39%
Low	0.0417	16%	0.0549	16%	32%

In addition, the canopy volumes data were analysed according to the differentiation of the three bands (low, mid and high band). In this case, the absolute frequency of partial canopy volumes was partitioned in intervals of 0.001 m^3 m^{-1} because of the lower canopy volume detected for single bands. Fig. 8 showed the data obtained in two different work sessions, corresponding to the BBCH 57 and BBCH 81 growth stage, and differentiated for single bands. The lower band is situated on the bottom of Fig. 8, and the others are above according to an increasing levels layout.
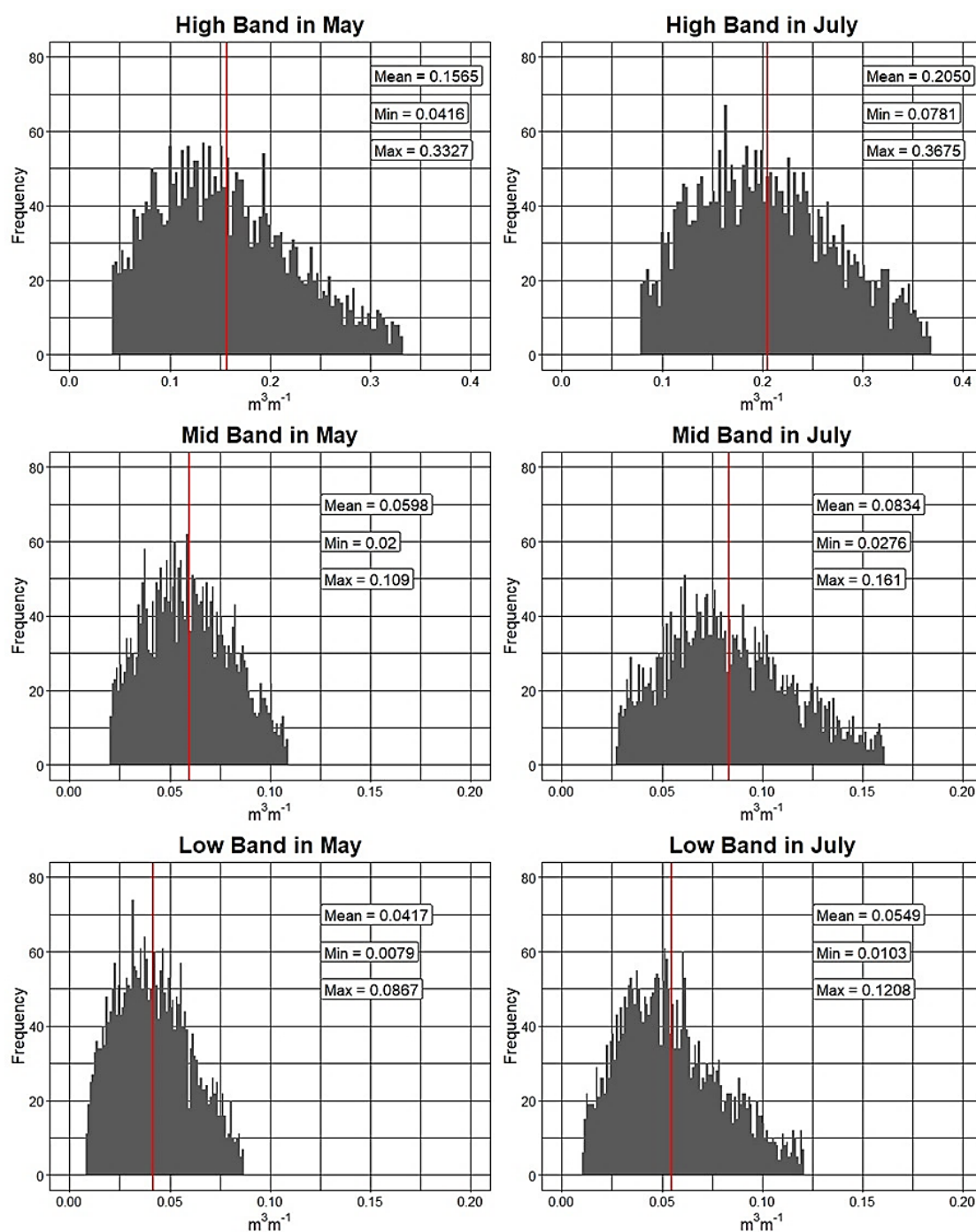
Figure 8. Absolut frequencies of LiDAR measurements of the three bands (Low, Mid, High) with an interval of 0.01 (m^3 m^{-1}). These measurements are part of software output (CSV file) where tractor, coupled with LiDAR, travelled completely four vine-rows. The red line corresponds to the mean value.

The graphs of low band canopy volumes showed that the average value of canopy volumes ranges from 0.042 m^3 m^{-1} to 0.055 m^3 m^{-1} during the growth stage (May–July), increasing 32%. A similar trend was highlighted for the other bands. The mid band ranges from 0.059 m^3 m^{-1} to 0.083 m^3 m^{-1}, with a volume increase of 39%, and the high

band goes from 0.156 m^3 m^{-1} to 0.205 m^3 m^{-1}, with a rise of 31% (Table 2) These increases prove that the software could also detect the growth of canopy volumes into the three bands between different moments of detections. The proportion of canopy distribution between bands seems not to change in the two different data collections.

CONCLUSIONS

The LiDAR-based algorithm and software for automated canopy volume calculation described in this work, can be a valid alternative to the complex and laborious procedures of canopy characteristics computing through post-processing points cloud reconstruction. The good correlations obtained between manual and LiDAR-based measurements ($R^2 = 0.67$, $R^2 = 0.74$) suggest that the simplified computing system can be a valuable tool for measuring canopy characteristics, such as tree row volume, and distinguishing the spatial canopy distribution.

The LiDAR-based algorithm showed good working adaptability on different vineyards vertical training systems, such as cordon training or Guyot, with different plant density. With inputs that can be set (row spacing, cordon height and LiDAR height) according to crop characteristics, the software for automatic canopy volume calculation can potentially be used in orchards.

The working conditions under which the software was tested are an indication that the LiDAR-based system can work at speeds similar to the on-farm management and spraying operations. Further tests will need to be carried out to fully investigate the best scanning frequency to achieve more accurate canopy volumes without compromising tractor working speed and efficiency. In addition, another interesting suggestion to evaluate further is the relation between canopy evaluation shown in this paper and canopy extraction in post-processing.

The results achieved in correlations between manual and LiDAR measurements take the work to the next stage of development. Firstly, it is necessary to check for bugs or other instrumental problems through a large number and lengthy field tests. Moreover, it will be about understanding how to best interact the data obtained from this system with the spraying equipment and spray volume.

In conclusion, the system (LiDAR, GNNS receiver, algorithm and software) has the potential to be implemented in precision viticulture both in on go variable-rate equipment and int on-board terminals based on prescription maps.

REFERENCES

Cheraïet, A., Naud, O., Carra, M., Codis, S., Lebeau, F. & Taylor, J. 2020. An algorithm to automate the filtering and classifying of 2D LiDAR data for site-specific estimations of canopy height and width in vineyards. *Biosystems Engineering* **200**, 450–465. doi: 10.1016/j.biosystemseng.2020.10.016

Comba, L., Biglia, A., Aimonino, D.R., Barge, P., Tortia, C. & Gay, P. 2019. 2D and 3D data fusion for crop monitoring in precision agriculture. In: *Proceedings of 2019 IEEE International Workshop on Metrology for Agriculture and Forestry (MetroAgriFor).* Portici, Italy, pp. 62–67. doi: 10.1109/MetroAgriFor.2019.8909219

Communication from the commission to the European Parliament, the Council, the European Economics and Social Committee and the Committee of the Regions. A Farm to Fork Stratsegy for a fair, healthy and environmentally-friendly food system. 2020. **COM/2020/381 final**, pp 19.

Directive 2009/128/EC of the European Parliament and the Council of 21 October 2009 establishing a framework for Community action to achieve the sustainable use of pesticides. 2009. *Official Journal of the European Union,* **L309**, 71–86.

EPRS (European Parliamentary Research Service). 2016. Precision agriculture and the future of farming in Europe. *European Parliamentary Research Service*, **PE 581.892**, pp. 40. https://ec.europa.eu/knowledge4policy/publication /precision-agriculture-future-farming-europe_en%0Ahttps://euagenda.eu/upload/publications/untitled-63196-ea.pdf

EPRS (European Parliamentary Research Service). 2017. Precision agriculture in Europe: Legal, social and ethical considerations. *European Parliamentary Research Service*, **PE 603.207**, pp. 80. http://www.europarl.europa.eu/RegData/etudes/STUD/2017/603207/EPRS_STU(2017)603207_EN.pdf

Gil, E., Llorens, J., Llop, J., Fàbregas, X., Escolà, A. & Rosell, J.R. 2013. Variable rate sprayer. Part 2 - Vineyard prototype: Design, implementation, and validation. *Computers and Electronics in Agriculture*, **95**, 136–150. doi: 10.1016/j.compag.2013.02.010

Llorens, J., Gil, E., Llop, J. & Escolà, A. 2010. Variable rate dosing in precision viticulture: Use of electronic devices to improve application efficiency. *Crop Protection* **29**(3), 239–248. doi: 10.1016/j.cropro.2009.12.022

Llorens, Jordi, Gil, E., Llop, J. & Escolà, A. 2011. Ultrasonic and LIDAR sensors for electronic canopy characterization in vineyards: Advances to improve pesticide application methods. *Sensors* **11**(2), 2177–2194. doi: 10.3390/s110202177

MIPAAF (Ministry of Agricultural, Food and Forestry Policies). 2014. National action plan for sustainable use of plant protection products. pp 83 (in Italian). https://www.mite.gov.it/sites/default/files/archivio/normativa/dim_22_01_2014.pdf

Miranda-Fuentes, A., Llorens, J., Rodríguez-Lizana, A., Cuenca, A., Gil, E., Blanco-Roldán, G.L. & Gil-Ribes, J.A. 2016. Assessing the optimal liquid volume to be sprayed on isolated olive trees according to their canopy volumes. *Science of the Total Environment* **568**, 296–305. doi: 10.1016/j.scitotenv.2016.06.013

Miranda-Fuentes, Antonio, Llorens, J., Gamarra-Diezma, J.L., Gil-Ribes, J.A. & Gil, E. 2015. Towards an optimized method of olive tree crown volume measurement. *Sensors* **15**(2), 3672–3687. doi: 10.3390/s150203671

Palacín, J., Pallejà, T., Tresanchez, M., Sanz, R., Llorens, J., Ribes-Dasi, M., Masip, J., Arnó, J., Escolà, A. & Rosell, J.R. 2007. Real-time tree-foliage surface estimation using a ground laser scanner. *IEEE Transactions on Instrumentation and Measurement* **56**(4), 1377–1383. doi: 10.1109/TIM.2007.900126

Pergher, G. & Petris, R. 2008. Pesticide dose adjustment to the canopy parameters for treatments to the tree crops. In: *Proceedings of Phytophatology Days*, pp. 317–322 (in Italian).

Román, C., Llorens, J., Uribeetxebarria, A., Sanz, R., Planas, S. & Arnó, J. 2020. Spatially variable pesticide application in vineyards: Part II, field comparison of uniform and map-based variable dose treatments. *Biosystems Engineering* **195**, 42–53. doi: 10.1016/j.biosystemseng.2020.04.013

Rosell, J.R. & Sanz, R. 2012. A review of methods and applications of the geometric characterization of tree crops in agricultural activities. *Computers and Electronics in Agriculture* **81**, 124–141. doi: 10.1016/j.compag.2011.09.007

Rosell, J.R., Llorens, J., Sanz, R., Arnó, J., Ribes-Dasi, M., Masip, J., Escolà, A., Camp, F., Solanelles, F., Gràcia, F., Gil, E., Val, L., Planas, S. & Palacín, J. 2009a. Obtaining the three-dimensional structure of tree orchards from remote 2D terrestrial LIDAR scanning. *Agricultural and Forest Meteorology* **149**(9), 1505–1515. doi: 10.1016/j.agrformet.2009.04.008

Rosell, J.R., Sanz, R., Llorens, J., Arnó, J., Escolà, A., Ribes-Dasi, M., Masip, J., Camp, F., Gràcia, F., Solanelles, F., Pallejà, T., Val, L., Planas, S., Gil, E. & Palacín, J. 2009b. A tractor-mounted scanning LIDAR for the non-destructive measurement of vegetative volume and surface area of tree-row plantations: A comparison with conventional destructive measurements. *Biosystems Engineering* **102**(2), 128–134. doi: 10.1016/j.biosystemseng.2008.10.009

Sanz, R., Rosell, J.R., Llorens, J., Gil, E. & Planas, S. 2013. Relationship between tree row LIDAR-volume and leaf area density for fruit orchards and vineyards obtained with a LIDAR 3D Dynamic Measurement System. *Agricultural and Forest Meteorology* **171–172**, 153–162. doi: 10.1016/j.agrformet.2012.11.013

Sarri, D., Lombardo, S., Pagliai, A., Zammarchi, L., Lisci, R. & Vieri, M. 2020. A technical-economic analysis of telemetry as a monitoring tool for crop protection in viticulture. *Journal of Agricultural Engineering* **51**(2), 91–99. doi: 10.4081/jae.2020.1029

Scapin, M.D.S., Behlau, F., Scandelai, L.H.M., Fernandes, R.S., Silva Junior, G.J. & Ramos, H. H. 2015. Tree-row-volume-based sprays of copper bactericide for control of citrus canker. *Crop Protection* **77**, 119–126. doi: 10.1016/j.cropro.2015.07.007

Tsoulias, N., Paraforos, D.S., Fountas, S. & Zude-Sasse, M. 2019. Estimating canopy parameters based on the stem position in apple trees using a 2D lidar. *Agronomy* **9**(11), 740. doi:10.3390/agronomy9110740

Zhang, Z., Wang, X., Lai, Q. & Zhang, Z. 2018. Review of Variable-Rate Sprayer Applications Based on Real-Time Sensor Technologies. In (book) *Automation in Agriculture - Securing Food Supplies for Future Generations* **i**(4), 53–79 doi: 10.5772/intechopen.73622